Annals of Biomedical Engineering, Vol. 40, No. 10, October 2012 *(© 2012)* pp. 2131–2139
DOI: 10.1007/s10439-012-0575-7

BMES BIOMEDICAL ENGINEERING SOCIETY™ www.bmes.org

Targeted Cancer Therapy by Immunoconjugated Gold–Gold Sulfide Nanoparticles Using Protein G as a Cofactor

XINGHUA SUN, GUANDONG ZHANG, DHRUVINKUMAR PATEL, DENNIS STEPHENS, and ANDRE M. GOBIN

Department of Bioengineering, University of Louisville, 419 Lutz Hall, Louisville, KY 40292, USA

(Received 27 January 2012; accepted 11 April 2012; published online 25 April 2012)

Associate Editor James Tunnell oversaw the review of this article.

Abstract—Gold–gold sulfide nanoparticles (GGS-NPs) fabricated from chloroauric acid and sodium thiosulfate show unique near infrared (NIR) absorption that renders them as a promising candidate for photothermal cancer therapy. To improve targeting efficiency, we developed a versatile method to allow ordered immunoconjugation of antibodies on the surfaces of these nanoparticles *via* a PEGylated recombinant Protein G (ProG). The PEGylated ProG was prepared with orthopyridyldisulfide-polyethylene glycol-succinimidyl valerate, average MW 2000 (OPSS-PEG-SVA), to first allow the self-assembly of ProG on the nanoparticles, subsequently antibodies were added to this construct to enable active targeting. The bioconjugated GGS-NPs were characterized by TEM, NIR-spectra, dynamic light scattering and modified immunoassay. In *in vitro* studies, the ProG-conjugated GGS-NPs with bound mouse anti c-erbB-2 (HER-2) immunoglobulin G (IgG) successfully targeted the HER-2 overexpressing breast cancer cell, SK-BR-3. Extensive cell death was observed for the targeted SK-BR-3 line at a low laser power of 540 J (3 W cm^{-2} for 3 min) while the control breast cancer cell (low expressing HER-2), HTB-22 survived. Using PEGylated ProG as a cofactor for immobilization of antibodies offers a promising strategy to functionalize various IgGs on nanoparticles for engineering their biomedical applications in cancer therapeutics.

Keywords—Gold nanoparticle, Cancer targeting, Bioconjugate, Protein G, Laser ablation, PEGylation.

ABBREVIATIONS

BSA	Bovine serum albumin
DI	Deionized
ELISA	Enzyme-linked immunosorbent assay
FBS	Fetal bovine serum
GGS	Gold-gold sulfide
GNP	Gold nanoparticle
HER-2	Human epidermal growth factor receptor-2 (c-erbB-2)
HRP	Horseradish peroxidase
IgG	Immunoglobulin G
mPEG	Monomethoxy polyethylene glycol
MWCO	Molecular weight cut-off
NIR	Near infrared
OD	Optical density
OPSS-PEG-SVA	Orthopyridyldisulfide-polyethylene glycol-succinimidyl valerate, average MW 2000
PEG	Polyethylene glycol
ProG	Protein G
PSG	Penicillin-streptomycin-glutamine
SEC	Size exclusion column
STD	Standard deviation
STEM	Scanning transmission electron microscope
TMB	3,3′,5,5′-tetramethylbenzidine dihydrochloride

Address correspondence to Andre M. Gobin, Department of Bioengineering, University of Louisville, 419 Lutz Hall, Louisville, KY 40292, USA. Electronic mail: andre.gobin@louisville.edu

INTRODUCTION

Metal nanoparticles (NPs) have currently attracted more and more research interest because of the innovative findings in both bioengineering and biomedical fields. Bioconjugated nanoparticles are one of the most interesting nanobiotechnology thrusts with respect to potential breakthroughs in both *in vitro* and *in vivo* applications.[3,11,26] As great building blocks for numerous nano architectures, protein-functionalized gold nanoparticles (GNPs) have been widely used in sensing, targeted delivery, imaging and therapy due to their unique properties such as surface plasmon resonance which can be tuned by precise fabrication for the desired GNP morphology.[8,21,28]

One essential optical characteristic that allows biomedical usage of GNPs such as silica-gold

nanoshells,[13,15,16] nanorods[17–19] and nanocages,[2,6,7] is the near infrared (NIR) resonance, which usually results from the unique morphology or geometry of GNP crystals. The significance of the NIR region to medicine is due to the high transmission and low absorption of light, between 650 and 900 nm, by native tissue components such as water and hemoglobin, enabling minimally invasive imaging and treatment modalities.[9,13,29] GNPs can be used to diagnose and photo-thermally treat tumors by localized hyperthermia with the combination of specific NIR lasers matching the peak resonance of the nanoparticles.[12,17,25] Considering the easy-fabrication properties, gold–gold sulfide nanoparticles (GGS-NPs) have been proven to be a promising early-stage diagnostic and photothermal therapeutic agent.[9,12] However, conjugating antibodies to the GGS-NPs plays a crucial role in active targeted imaging and therapy. For the greatest efficacy, the antibody immobilized on GGS-NPS should retain its optimal activity toward the antigen after the conjugation. To improve the targeting efficiency, a suitable conjugation strategy focusing on specific proteins and GNPs needs to be carefully considered. There are usually three key strategies for bioconjugation to GNPs: physical adsorption (by hydrophobic or electrostatic interaction), covalent immobilization, and specific binding using a cofactor.[3,26] For each method, denaturation and orientation of the protein on the solid surfaces are critical to their subsequent application.[11,27] The ideal immobilization of antibodies on GNPs is by the F_c region with their antigen recognition sites (F_{ab} regions) easily accessible to the targeted antigens.

Protein G (ProG) is a group C and G *Streptococcal* bacteria-expressing protein capable of specifically binding to an immunoglobulin (Ig) at the constant F_c region, and recombinant ProG short of albumin-binding domains can be genetically expressed in *E. coli*.[1,14] This specific antibody-binding ability of recombinant ProG makes it a great candidate exploited as a cofactor to engineer a versatile bio-conjugated NP for antibody capture with maximal antigen-binding activity. ProG has a strong binding affinity to immunoglobulin G (IgG), especially to mouse IgGs. Binding the recombinant ProG that has no free-thiol groups to GNPs through physical adsorption leads to random coating and partial IgG-binding activity loss. More ordered immobilization of antibodies on GNPs can be achieved by pre-coating a genetically modified ProG with a cysteine tail to gold surfaces or more complex ProG-DNA conjugates.[10,22,23]

In this work, we attached a bi-functional PEG to ProG for the immobilization of ProG on the GGS-NPs with NIR absorption at around 860 nm. These nanoparticles were prepared from a simple reaction between chloroauric acid and sodium thiosulfate that we have previously reported.[30] The PEG-ProG conjugated GNPs are stable in a variety of saline environments used to evaluate the targeting. ProG was PEGylated with orthopyridyldisulfide-polyethylene-glycol-succinimidyl valerate, average MW 2000 (OPSS-PEG-SVA), and subsequently conjugated these to the nanoparticle surface. The ProG-PEG-GGS-NPs were then used to immobilize IgGs, by the F_c region, for recognizing the antigens on the targeted cell membranes for further laser therapy. The aim was to be able to develop a platform for the immobilization of various IgGs for targeted therapy of different cells as shown in Fig. 1, rather than attaching a specific antibody to the nanoparticle, increasing versatility of the system. Two human breast cancer cell lines were utilized. SK-BR-3 cells, that overexpress human epidermal growth factor receptor-2 (c-erbB-2 or HER-2), and HTB-22 cells with low HER-2 expression were selected as the positive target and negative control, respectively. SK-BR-3 cells were

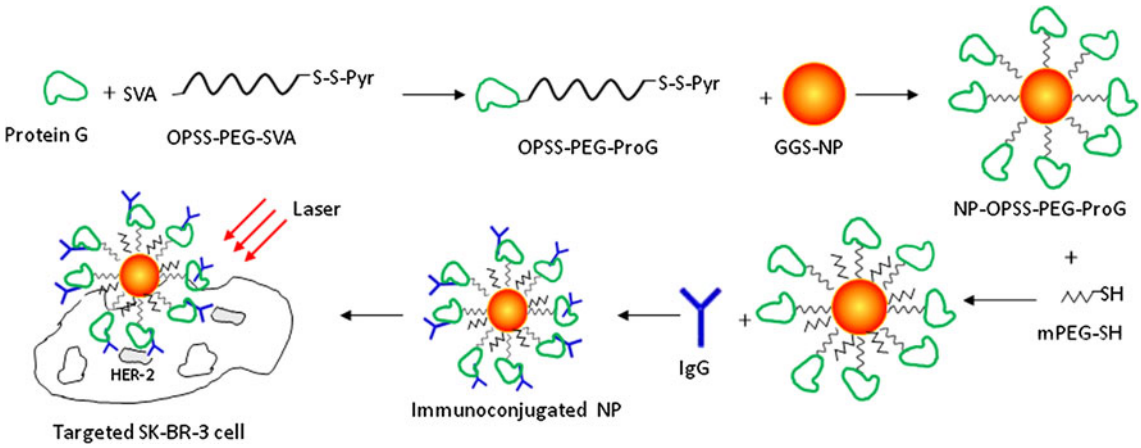

FIGURE 1. The schematic strategy of the PEGylation of ProG with OPSS-PEG-SVA and targeted therapy of breast cancer using the immunoconjugated GGS-NPs *via* ProG.

efficiently targeted and ablated by the as-prepared immunoconjugated GGS-NPs at the suitable conditions.

MATERIALS AND METHODS

Materials

Hydrogen tetrachloroaurate(III) trihydrate was purchased from Alfa Aesar (36400, Ward Hill, MA). Sodium thiosulfate (380016), 3,3′,5,5′-tetramethylbenzidine dihydrochloride (TMB, T3405), hydrogen peroxide solution (H3410), bovine serum albumin (BSA, A7906), Bradford reagent (B6916), monoclonal anti-HER-2 antibody produced in mouse (E2777), recombinant Protein G (P4689, MW 21600), and anti mouse IgG-peroxidase produced in goat (A4416) were all purchased from Sigma-Aldrich (St. Louis, MO). Fetal bovine serum (FBS) was purchased from Atlanta Biologics (Lawrenceville, GA). Penicillin–streptomycin-glutamine (PSG) solution was purchased from Thermo Scientific (Logan, UT). Orthopyridyldisulfide-polyethylene glycol-succinimidyl valerate, average MW2000 (OPSS-PEG-SVA) and mPEG-SH (MW1000) were purchased from Laysan Bio (Arab, AL). McCoy's 5A modified medium (McCoy) and Minimum essential medium eagle (EMEM) were purchased from ATCC (Manassas, VA). Deionized (DI) water used was 18.2 MΩ cm (Thermo Scientific).

GGS-NP Synthesis and Characterization

GGS-NPs with NIR resonance were synthesized by directly adding 3 mM $Na_2S_2O_3$ solution into 1.7 mM $HAuCl_4$ solution with the volumetric ratio of 2.8 ($HAuCl_4$:$Na_2S_2O_3$) and gently shaken for 15 s then allowed to react for 1 h. The as-synthesized GGS-NPs were then centrifuged (1200×*g* for 20 min) to remove most of the gold colloid by-products and increase purity of the NIR absorbing fraction of nanoparticles.[12] The pellets were collected and the corresponding supernatants were spun down again to increase yield. This method of purification by centrifugation was performed three times.

The optical properties of GNPs were characterized using a UV–Visible–IR spectrophotometer (Cary-50, Varian, Walnut Creek, CA), and the size and zeta potential were measured using a Zetasizer (Nano-ZS90, Malvern). A FEI Tecnai F20 transmission electron microscope (TEM) operated at 200 kV was used to determine the shape and size of GNPs. The TEM samples were prepared by dropping 20 μL of gold particle suspension in DI water onto Holey carbon film enhanced TEM grids (C-flat) followed by a room temperature drying.

PEGylation and Conjugation of Protein G on GGS-NPs

ProG was PEGylated by OPSS-PEG-SVA using a modification of the method reported by Chattopadhyay *et al.*[5] Briefly, 0.5 mL of ProG (1 mg mL^{-1}) in pH 7.4 PBS was mixed with 0.5 mL of OPSS-PEG-SVA in 100 mM $NaHCO_3$ solutions to achieve molar ratios of 1:10 and 1:25 (ProG:OPSS-PEG-SVA) and was magnetically stirred for 3 h at room temperature. The mixture was then stored overnight at 4 °C. The products were purified to remove unreacted PEG using membrane ultrafiltration (10 kDa MWCO, Pall, Ann Arbor, MI). The purified PEGylated ProG was collected into 10 mM phosphate buffer, pH 7.4 and the concentration was assayed using Bradford reagent with suitable dilution range. The conjugation efficiency was analyzed in a size exclusion column (SEC, Superose 12, GE Healthcare Bioscience) equipped in a Waters HPLC system (Milford, MA). Samples were eluted using PBS consisting of 10 mM phosphate, 10 mM KCl and 140 mM NaCl at flow rate of 0.3 mL min^{-1}.

To conjugate the cofactor, ProG to GGS-NPs, the bare GGS-NPs dispersed in DI water were first mixed with the PEGylated ProG at a molar ratio of 500:1 (ProG:NP) on an orbital rotator (Boekel Scientific, Feasterville, PA) for 1 h at room temperature and continuing overnight at 4 °C. To then block any remaining exposed gold surface, mPEG-SH (MW1000) was added to the conjugated nanoparticles at a molar ratio of 500:1 (mPEG-SH:NP) overnight at 4 °C. The ProG-conjugated NPs were then centrifuged twice at 2000×*g* for 20 min to remove the excess ProG and mPEG. Lastly, pellets were re-dispersed in PBS at a desired optical density.

The IgG captured by ProG-conjugated GGS nanoparticles was quantitatively assayed by modifying the ELISA reported by Day *et al.*[9] Briefly, ProG-conjugated nanoparticles were first incubated with anti-HER-2 IgGs at a molar ratio of 200:1 (IgG:NP) for 20 min at room temperature and centrifuged twice at 2000×*g* for 20 min to remove unbound antibodies. The GGS-NP-PEG-ProG-anti HER-2 and control (mPEG-SH only) nanoparticles were incubated with 100 μg mL^{-1} horseradish peroxidase (HRP)-conjugated goat anti-mouse IgG in 3% solution of BSA in PBS (PBSA) for 1 h at room temperature. The nanoparticles were centrifuged twice at 2000×*g* for 7 min to remove the excess HRP-conjugated anti-mouse IgGs and the pellets were re-suspended in PBSA. The HRP-bound GNPs were developed using TMB with H_2O_2 for 15 min and the reaction was stopped by the addition of 2 M sulfuric acid. The count of anti-mouse IgG was calculated by comparison to a standard absorption curve of the appropriate HRP-conjugated anti-mouse IgG at 450 nm. The concentration of

nanoparticles was calculated from the Beer–Lambert law with the extinction coefficient of GGS-NPs derived from Mie theory as described by Averitt *et al.*[4]

Cell Culture and Laser Ablation

HER-2 overexpressing SK-BR-3 and control HTB-22 carcinoma cells were cultured in a 75 cm^2 (T-75) flasks using McCoy containing 10% FBS and 1% PSG, and EMEM containing 10% FBS, 1% PSG and 0.1% insulin, respectively. When cells were confluent, they were detached by Trypsin-EDTA (Mediatech, Manassas, VA). 50 μL of the cell suspension per well was then seeded with 1 mL cell media in a flat bottom 24-well microplate (353047, Becton, Franklin Lakes, NJ) to facilitate efficient laser irradiation by alternating plates thus subjecting cells to minimal disturbances in environment. Cells in wells were cultured at 5% CO_2 in an incubator for ~3 days prior to exposure to laser light at 3 W cm^{-2}.

When the cells were 80% confluent, the cell media was removed and the adherent cells were washed with PBS. A suspension of GGS-NP-PEG-ProG was incubated with anti-HER-2 antibody at the optical intensity of 3.5 OD (~6.8 × 10^{11} particles mL^{-1}) at a molar ratio of 60:1 (anti-HER-2:NP) for 20 min at room temperature. 0.5 mL of antibody-conjugated GGS-NPs were then pipetted into each well. After incubation for 60 min, the GNP suspension was removed and cells were thoroughly washed with PBS. 0.3 mL of cell media was pipetted into each well and the cells were irradiated with an 817 nm laser (Coherent, Santa Clara, CA) using designed power by controlling power density and duration. The same ablation power was performed in multiple wells to establish repeatability in the procedure as assayed by staining.

The cells were incubated overnight and rinsed with PBS and tested for cell viability/cytotoxicity using a live/dead cell assay kit (Invitrogen, Eugene, OR). 0.5 mL of assay PBS solution consisting of 0.5 μL of Calcein AM and 1 μL of Ethidium homodimer-1 (EthD-1) was pipetted into each well and incubated for 30 min. The cells were then rinsed with PBS and imaged using an Accu-scope 3032 fluorescence microscope (New York Microscope, Hicksville, NY) equipped with a Nikon Sight DS-Qi/Mc digital camera (Nikon instruments, Melville, NY). Images were analyzed using NIS-Elements AR 3.2 software (Nikon instruments). Calcein AM stains live cells fluorescent green while EthD-1 stains dead cells fluorescent red.

Silver Enhancement Stain

To assist the observation of the binding of nanoparticles on the targeted cells, cells incubated with the bioconjugated GGS-NPs were stained using a silver-enhancement stain at the same time as the laser ablation study in parallel wells. After the binding of GNPs, cells were washed three times with PBS, and were stained using a silver-enhancer kit that bound to GNPs (enhancer A and B, Sigma). The stained cells bound with GGS-NPs were fixed using 10% buffered formalin solution (SF100-4, Fisher Scientific, Fair lawn, NJ) for 6 min and pictures were taken using a Olympus CKX41 microscopic equipped with a Nikon D90 camera.

RESULTS

Figure 2 shows the typical SEC-HPLC chromatograms of the ultrafiltrated PEGylated ProG at two different molar ratios of 10:1 and 25:1 (OPSS-PEG-SVA:ProG). Compared with the intact recombinant ProG, the peaks of the PEGylated ProG were shifted to the large molecule side (eluted earlier from the SEC). This shift indicates that the OPSS-PEGs were efficiently coupled to ProG by an amide bond, providing disulfide groups for the interaction with gold surfaces. Higher molar ratio of OPSS-PEG-SVA to ProG resulted in more PEG molecules attached per ProG molecule.

As shown in Fig. 3e, the as-synthesized bare GGS-NPs have a NIR absorption peak at about 860 nm with a weak accompanying peak at 530 nm. Scanning TEM (STEM) images confirmed that the controlled NIR absorption at 860 nm was due to the multiple shapes of GGS-NP crystals such as truncated polyhedra, triangle nanoplates and nanorods (Figs. 3a, 3c). After ProG conjugation and purification, the NIR absorption peak slightly red-shifted in wavelength and

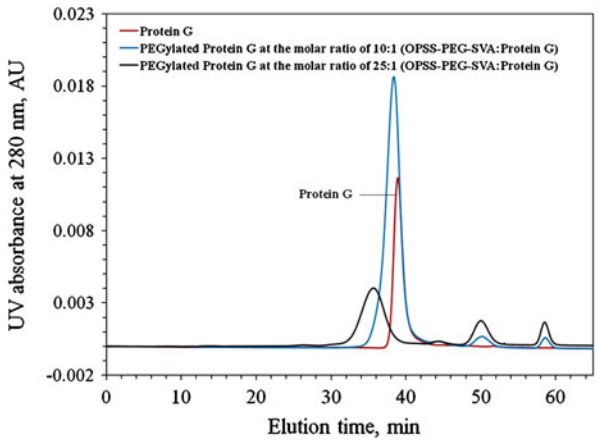

FIGURE 2. SEC-HPLC chromatograms of the PEGylated ProG with OPSS-PEG-SVA at two different molar ratios of OPSS-PEG-SVA to ProG: 10:1 and 25:1. ProG was used for comparison with PEGylated ProG. The elution buffer was pH 7.4 PBS consisting of 5 mM phosphates, 10 mM KCl and 140 mM NaCl. The elution flow rate was 0.3 mL min^{-1}.

~5 nm PEGylated ProG layer was observed around some of the GGS-NPs (Figs. 3b, 3d).

Compared with the bare GGS-NPs, the NIR absorption, hydrodynamic diameter and zeta potential of bioconjugated GNPs were all changed. The data is summarized in Table 1. The modified ELISA used to determine the number of anti-HER-2 IgG captured by immobilized ProG showed 52.0 ± 7.4 IgGs per particle for ProG-conjugated GGS-NPs while 4.0 ± 0.4 IgGs per particle for mPEG-SH blocked particles. This data supports that the conjugated ProG on NP retains the activity to capture mouse anti-HER-2 IgGs.

Immunohisto-staining on the HER-2 overexpressing human breast cancer cells used in this work showed a high positive result for SK-BR-3 with low HER-2 expressed by control cell of HTB-22 (data are not shown). Figure 4 shows the silver enhancement stain images using HTB-22 and ProG-conjugated GGS-NP as the negative controls for cancer cell and nanoparticles, respectively. Higher nanoparticle binding on the HER-2 overexpressing SK-BR-3 cells is indicated by increased silver enhancement, suggesting the recognition of the anti-HER-2 IgG conjugated by the GNP-ProG to HER-2. In contrast, there is lower enhancement (lighter staining) where fewer particles are bound on both control samples.

Figure 5 shows the cell viability after laser ablation of cells incubated with the antibody conjugated GGS-NPs. It is seen that 3 W cm^{-2} laser density and 3 min exposure (540 J) killed HER-2 overexpressing SK-BR-3 cells. Lower power, 3 W cm^{-2} for 2 min (360 J) showed poor ablation efficiency.

As a control, high viability of HTB-22 cells with less HER-2 expression was observed at the 540 J (3 W cm^{-2} for 3 min) treatment. Another negative control using PBS also gave high cell viability as a result of 540 J exposure. This suggests evidence for the targeted delivery of GGS-NPs to SK-BR-3 cells and cell-specific ablation. For the ProG-conjugated GGS-NPs with no anti-HER-2 IgGs, both SK-BR-3 and HTB-22 cells decreased viability by 10–20% as some ProG-conjugated GGS-NPs might have attached to cells due to nonspecific binding.

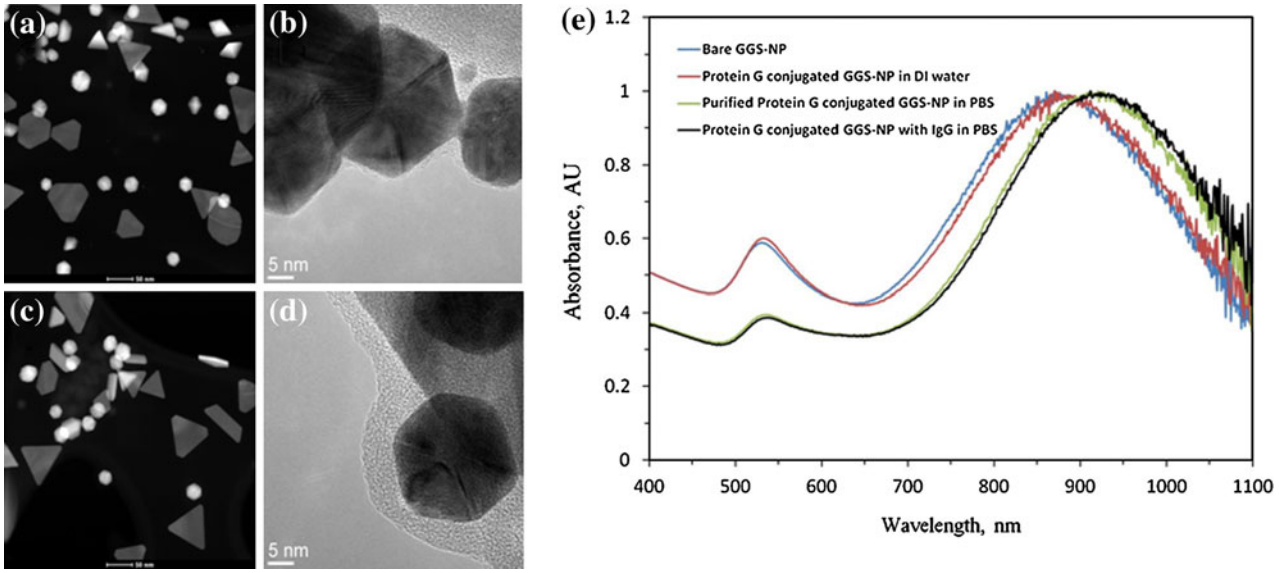

FIGURE 3. STEM (a, c) and high resolution TEM (b, d) images of the bare GGS-NPs and ProG-conjugated GGS-NPs: (a) and (b) Bare GGS-NPs. (c) and (d) Purified ProG-conjugated GGS-NPs. The NIR spectra of the bare and bioconjugated GGS-NPs (e).

TABLE 1. Changes in the parameters of GGS-NPs before and after the bioconjugation.

	Bare GGS-NP	Unpurified GGS-NP-PEG-ProG in DI water	Purified GGS-NP-PEG-ProG in PBS	GGS-NP-PEG-ProG-anti HER-2 IgG
NIR absorbance, nm	861 ± 16	874 ± 14	887 ± 23	889 ± 28
Diameter, nm	47.4 ± 4.7	73.6 ± 5.0	71.4 ± 5.3	87.8 ± 7.3
Zeta potential, mV	−48.3 ± 2.9	−23.8 ± 4.5	−9.0 ± 1.8	−3.5 ± 2.9

The bare GGS-NPs were suspended in DI water while the conjugated ones were in DI water or PBS. Data were given in mean ± STD for three batch samples.

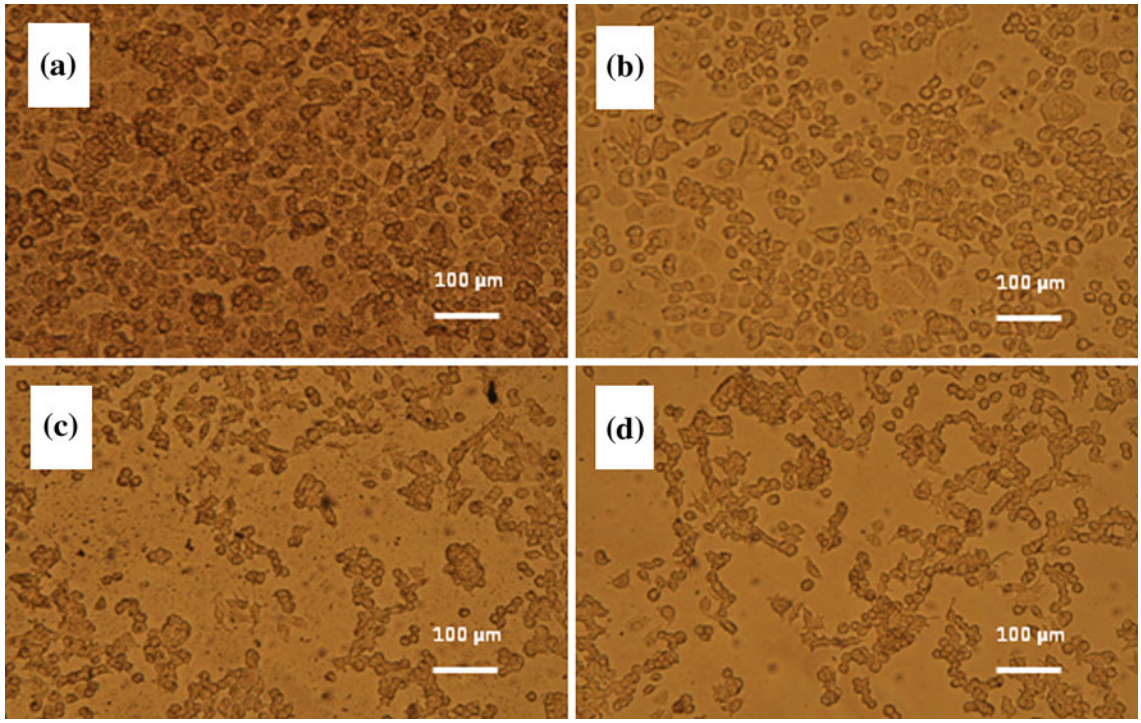

FIGURE 4. Images of the silver-enhancement stain of SK-BR-3 and HTB-22 cancer cells incubated with the GGS-NP-OPSS-PEG-ProG with immobilized anti-HER-2 IgGs. (a) SK-BR-3 with GGS-NP-OPSS-PEG-ProG-anti HER-2 IgG. (b) SK-BR-3 with GGS-NP-OPSS-PEG-ProG. (c) HTB-22 with GGS-NP-OPSS-PEG-ProG-anti HER-2 IgG. (d) HTB-22 with GGS-NP-OPSS-PEG-ProG.

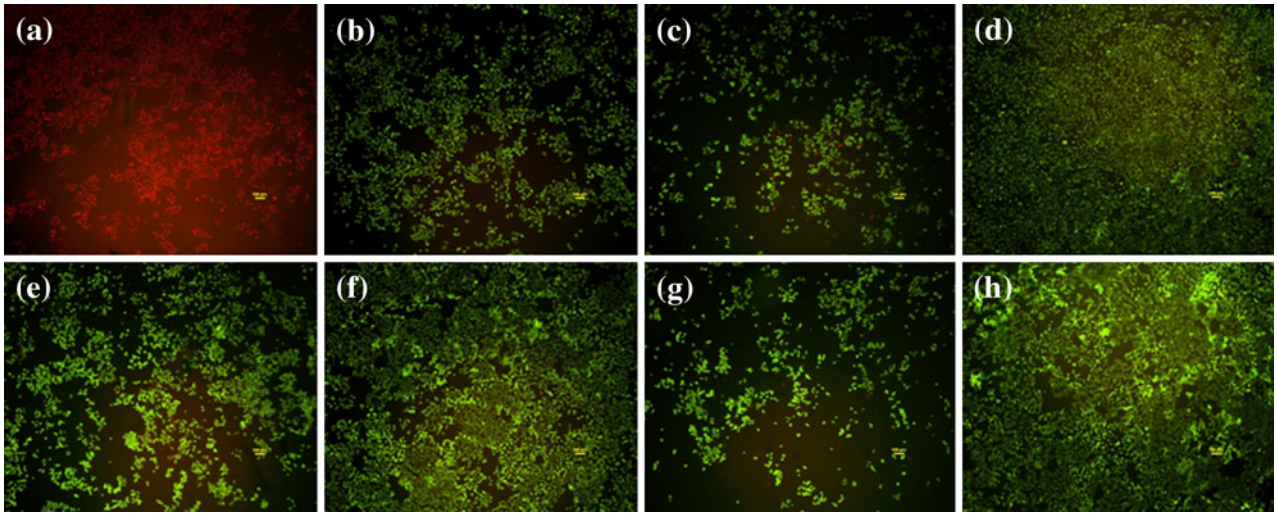

FIGURE 5. Live/dead assay images of SK-BR-3 (a–d) and HTB-22 (e–h) cancer cells after laser ablation with different operation conditions. (a) SK-BR-3 with GGS-NP-OPSS-PEG-ProG-anti HER-2 IgG at 540 J. (b) SK-BR-3 with GGS-NP-OPSS-PEG-ProG-anti HER-2 IgG at 360 J. (c) SK-BR-3 with GGS-NP-OPSS-PEG-ProG at 540 J. (d) SK-BR-3 with PBS at 540 J. (e) HTB-22 with GGS-NP-OPSS-PEG-ProG-anti HER-2 IgG at 540 J. (f) HTB-22 with GGS-NP-OPSS-PEG-ProG-anti HER-2 IgG at 360 J. (g) HTB-22 with GGS-NP-OPSS-PEG-ProG at 540 J (h) HTB-22 with PBS at 540 J. Green stain shows live cells and red, dead ones. All scale bars represent 100 microns, 3 W cm^{-2} for 3 min equals to 540 J.

DISCUSSION

Recombinant ProG is a small single chain protein (21.6 kDa) lacking the albumin binding regions, and has much stronger binding affinity to mouse IgGs than Protein A. Since the anti-HER-2 IgG used in the present targeting is mouse IgG1, the recombinant ProG is an ideal cofactor for the preparation of immunoconjugated GGS-NPs by immobilization of

anti-HER-2 IgG through its constant F_c region. This specifically oriented binding of IgGs may retain the activity of the immobilized IgGs to the HER-2 overexpressed in SK-BR-3 cell membranes. As the recombinant ProG is short of free thiol residues, a PEG linker with disulfide group is induced to ProG molecule by the modification of the alpha-amine on the lysine residues of ProG. There are two advantages of the PEGylation: assistance of the immobilization of ProG on the gold surfaces through the disulfide group of OPSS-PEG, and isolation of ProG from GNP surface avoiding loss of the activity of IgG capture region. Considering the binding of ProG to various IgGs, cancer diagnosis and targeted therapy by immunoconjugated GGS-NPs *via* ProG provides a repeatable platform method for antibody conjugation to gold nanoparticles.

The molar ratio of OPSS-PEG-SVA to ProG was optimized to be 25 in this work as it was observed that high molar ratio was related to PEGylated ProG precipitation during the membrane ultrafiltration with possible IgG-binding activity loss of ProG due to the complex conformation change (especially the IgG binding regions) of the ProG molecule. The PEG-ProG conjugated GGS-NPs showed good stability in PBS.

The unique NIR resonance qualifies the GGS-NPs as an ideal reagent for targeted therapy with less-invasive and deep-penetrative laser radiation at 817 nm. From the STEM images, as shown in Fig. 3, the shapes of the NPs were not affected by centrifugation but more of the smaller spherical particles were removed. High resolution TEM images of bare GNPs indicated that a very thin chemical layer (<2 nm) is present around the GGS-NPs to stabilize the gold crystals. In contrast, a much thicker layer of PEGylated ProG (>5 nm) around the conjugated GGS-NPs was clearly observed, demonstrating the successful self-assembly of PEGylated ProG on NPs. This result was in good agreement with the stability of the conjugated GGS-NPs in salt solution, while the bare GNPs showed very poor stability.

Significant changes of characteristic parameters among the bioconjugated GGS-NPs were found. The absorption peak wavelength shift of ~10–20 nm after the ProG conjugation and purification could be related to PEG-ProG layer coated around particles, and the purification steps that removed more spherical NPs from the ProG-conjugated samples at 2000 × *g*. With the 2 KDa OPSS-PEG (Stokes diameter ~6.5 nm) linked onto ~7 nm ProG,[1,5] the ~25 nm increase in diameter demonstrated good attachment of PEGylated ProG to GGS-NPs.[20,24] The remarkable drop in charge density characterized by zeta potential also proved the successful conjugation of PEGylated ProG on the gold surface through the disulfide groups. The ProG coated NPs showed a difference in zeta potential between DI and PBS which could be the result of the ProG charge shift in a different pH and ionic environment as is common with proteins. Further, the change in charge continues in the same direction as the IgG is attached to form the final construct showing that larger diameter shields more of the negative charge of the gold nanoparticle.

The parameter changes of the GGS-NPs with bound IgGs (shown in Table 1) also demonstrated that the immobilization of anti-HER-2 IgGs was achieved *via* the capture of ProG on the particles. The ~15 nm increase in diameter indicated the orientated binding of IgGs to the PEGylated ProG immobilized on GGS-NPs. The further decrease in charge density was related to the neutral pH of PBS that was near the isoelectric point of IgG. The promise of the versatility of the layered approach on GNPs for multi-targeting tasks using various antibodies was possible.

Using the silver enhancement stain, the comparison showed that more immunoconjugated GNPs were attached to SK-BR-3 cells. Both SK-BR-3 cells and HTB-22 cells showed weak interaction to ProG-conjugated GGS-NPs with no bound anti-HER-2 IgGs. This strongly confirms the activity of captured IgG to its antigen, validating the potential utilization of the immunoconjugated GGS-NPs as therapeutic agents for targeted breast cancer treatments.

Serious death of SK-BR-3 cells caused by 540 J (3 W cm^{-2} for 3 min) laser ablation, as shown in Fig. 5, proved our hypothesis of the targeted photothermal cancer therapy using immunoconjugated GGS-NPs *via* the PEGylated ProG. It should be noted that some HTB-22 cells were found dead after the laser ablation at 540 J. This can be explained by the differential expression levels of HER-2 in this cell line. There are two known possible mechanisms for the interaction between GNP and cells in localized photothermal cancer therapy: NP attachment on cellular membranes or NP uptake by cells. Under laser exposure, the GNPs attached on cell membranes cause thermal damage of the membrane, leading to cytoplasmic leakage and cell death.[15] However, internalized GNPs can result in cell death related to DNA damage. We are continuing to investigate to see which mechanism is dominant for our immunoconjugated GGS-NPs, assisting us to understand the fundamentals of photothermal ablation and inspiring new thermal drug delivery method using the ProG-conjugated GGS-NPs.

CONCLUSIONS

Immunoconjugated GNPs using a cofactor is of importance to the preparation of versatile GNP

platform for targeted therapy. The present conjugation of the PEG-ProG on the GGS-NPs fabricated from chloroauric acid and sodium thiosulfate offers a practical protocol. In *in vitro* studies, the as-fabricated ProG-conjugated GGS-NPs with bound mouse monoclonal anti-erbB-2 (HER-2) IgGs were found to target at HER-2 overexpressing breast cancer cell line, SK-BR-3 and showed almost total ablation at the selected laser power of 540 J (3 W cm^{-2} over 3 min) while most HTB-22 cells with low HER-2 expression survived. The unique NIR absorption of GNPs and the versatile antibody binding ability of the conjugated ProG demonstrated the proof-of-concept of photothermal cancer therapy using immunoconjugated GGS-NPs *via* PEG-ProG.

ACKNOWLEDGMENTS

This work was funded by the grant from Wallace Coulter Foundation: Early Career Phase I award, and NSF-EPSCoR No. 0814194. XS would like to express acknowledge to Marty O'Toole in Bioengineering at the University of Louisville for the assistant on HPLC analysis.

CONFLICT OF INTEREST

The authors state that they have no conflicts of interest.

REFERENCES

[1]Akerstrom, B., and L. Bjorck. A physicochemical study of Protein-G, a molecule with unique immunoglobulin-G-binding properties. *J. Biol. Chem*. 261:240–247, 1986.

[2]Au, L., Q. Zhang, C. M. Cobley, M. Gidding, A. G. Schwartz, J. Y. Chen, and Y. N. Xia. Quantifying the cellular uptake of antibody-conjugated Au nanocages by two-photon microscopy and inductively coupled plasma mass spectrometry. *ACS Nano* 4:35–42, 2010.

[3]Aubin-Tam, M. E., and K. Hamad-Schifferli. Structure and function of nanoparticle-protein conjugates. *Biomed. Mater*. 3:034001, 2008.

[4]Averitt, R. D., S. L. Westcott, and N. J. Halas. Linear optical properties of gold nanoshells. *J. Opt. Soc. Am. B-Opt. Phys*. 16:1824–1832, 1999.

[5]Chattopadhyay, N., Z. L. Cai, J. P. Pignol, B. Keller, E. Lechtman, R. Bendayan, and R. M. Reilly. Design and characterization of HER-2-targeted gold nanoparticles for enhanced X-radiation treatment of locally advanced breast cancer. *Mol. Pharm*. 7:2194–2206, 2010.

[6]Chen, J., F. Saeki, B. J. Wiley, H. Cang, M. J. Cobb, Z. Y. Li, L. Au, H. Zhang, M. B. Kimmey, X. D. Li, and Y. Xia. Gold nanocages: bioconjugation and their potential use as optical imaging contrast agents. *Nano Lett*. 5:473–477, 2005.

[7]Chen, J. Y., B. Wiley, Z. Y. Li, D. Campbell, F. Saeki, H. Cang, L. Au, J. Lee, X. D. Li, and Y. N. Xia. Gold nanocages: engineering their structure for biomedical applications. *Adv. Mater*. 17:2255–2261, 2005.

[8]Daniel, M. C., and D. Astruc. Gold nanoparticles: assembly, supramolecular chemistry, quantum-size-related properties, and applications toward biology, catalysis, and nanotechnology. *Chem. Rev*. 104:293–346, 2004.

[9]Day, E. S., L. R. Bickford, J. H. Slater, N. S. Riggall, R. A. Drezek, and J. L. West. Antibody-conjugated gold–gold sulfide nanoparticles as multifunctional agents for imaging and therapy of breast cancer. *Int. J. Nanomed*. 5:445–454, 2010.

[10]Fowler, J. M., M. C. Stuart, and D. K. Y. Wong. Self-assembled layer of thiolated protein G as an immunosensor scaffold. *Anal. Chem*. 79:350–354, 2007.

[11]Gagner, J. E., M. D. Lopez, J. S. Dordick, and R. W. Siegel. Effect of gold nanoparticle morphology on adsorbed protein structure and function. *Biomaterials* 32:7241–7252, 2011.

[12]Gobin, A. M., E. M. Watkins, E. Quevedo, V. L. Colvin, and J. L. West. Near-infrared-resonant gold/gold sulfide nanoparticles as a photothermal cancer therapeutic agent. *Small* 6:745–752, 2010.

[13]Gobin, A. M., M. H. Lee, N. J. Halas, W. D. James, R. A. Drezek, and J. L. West. Near-infrared resonant nanoshells for combined optical imaging and photothermal cancer therapy. *Nano Lett*. 7:1929–1934, 2007.

[14]Guss, B., M. Eliasson, A. Olsson, M. Uhlen, A. K. Frej, H. Jornvall, J. I. Flock, and M. Lindberg. Structure of the IGG-binding regions of streptococcal Protein-G. *EMBO J*. 5:1567–1575, 1986.

[15]Hirsch, L. R., A. M. Gobin, A. R. Lowery, F. Tam, R. A. Drezek, N. J. Halas, and J. L. West. Metal nanoshells. *Ann. Biomed. Eng*. 34:15–22, 2006.

[16]Hirsch, L. R., R. J. Stafford, J. A. Bankson, S. R. Sershen, B. Rivera, R. E. Price, J. D. Hazle, N. J. Halas, and J. L. West. Nanoshell-mediated near-infrared thermal therapy of tumors under magnetic resonance guidance. *Proc. Natl Acad. Sci. USA*. 100:13549–13554, 2003.

[17]Huang, X. H., P. K. Jain, I. H. El-Sayed, and M. A. El-Sayed. Gold nanoparticles: interesting optical properties and recent applications in cancer diagnostic and therapy. *Nanomedicine* 2:681–693, 2007.

[18]Huang, X. H., S. Neretina, and M. A. El-Sayed. Gold nanorods: from synthesis and properties to biological and biomedical applications. *Adv. Mater*. 21:4880–4910, 2009.

[19]Jain, P. K., K. S. Lee, I. H. El-Sayed, and M. A. El-Sayed. Calculated absorption and scattering properties of gold nanoparticles of different size, shape, and composition: applications in biological imaging and biomedicine. *J. Phys. Chem. B* 110:7238–7248, 2006.

[20]Jans, H., X. Liu, L. Austin, G. Maes, and Q. Huo. Dynamic light scattering as a powerful tool for gold nanoparticle bioconjugation and biomolecular binding Studies. *Anal. Chem*. 81:9425–9432, 2009.

[21]Jones, M. R., R. J. Macfarlane, B. Lee, J. A. Zhang, K. L. Young, A. J. Senesi, and C. A. Mirkin. DNA-nanoparticle superlattices formed from anisotropic building blocks. *Nat. Mater*. 9:913–917, 2010.

[22]Jung, Y., J. M. Lee, H. Jung, and B. H. Chung. Self-directed and self-oriented immobilization of antibody

by protein G-DNA conjugate. *Anal. Chem.* 79:6534–6541, 2007.
[23]Lee, J. M., H. K. Park, Y. Jung, J. K. Kim, S. O. Jung, and B. H. Chung. Direct immobilization of protein G variants with various numbers of cysteine residues on a gold surface. *Anal. Chem.* 79:2680–2687, 2007.
[24]Liu, Y. L., M. K. Shipton, J. Ryan, E. D. Kaufman, S. Franzen, and D. L. Feldheim. Synthesis, stability, and cellular internalization of gold nanoparticles containing mixed peptide-poly(ethylene glycol) monolayers. *Anal. Chem.* 79:2221–2229, 2007.
[25]Lowery, A. R., A. M. Gobin, E. S. Day, N. J. Halas, and J. L. West. Immunonanoshells for targeted photothermal ablation of tumor cells. *Int. J. Nanomed.* 1:149–154, 2006.
[26]Rana, S., Y. C. Yeh, and V. M. Rotello. Engineering the nanoparticle-protein interface: applications and possibilities. *Curr. Opin. Chem. Biol.* 14:828–834, 2010.
[27]Sun, X. H., D. Q. Yu, and R. Ghosh. Study of hydrophobic interaction based binding of immunoglobulin G on synthetic membranes. *J. Membr. Sci.* 344:165–171, 2009.
[28]Sun, Y. G., and Y. N. Xia. Shape-controlled synthesis of gold and silver nanoparticles. *Science* 298:2176–2179, 2002.
[29]Weissleder, R. A clearer vision for in vivo imaging. *Nat. Biotechnol.* 19:316–317, 2001.
[30]Zhang, G. D., J. Jasinski, D. Patel, K. James, X. H. Sun, and A. M. Gobin. Near infrared tunable gold nanoparticles for low power laser ablation of esophageal adenocarcinoma. In: *Proceedings of MRS 2011 fall meeting*, 2011.